Petr Sváček

Numerical simulation of free-surface flows with surface tension

In: Jan Chleboun and Petr Přikryl and Karel Segeth and Jakub Šístek and Tomáš Vejchodský (eds.): Programs and Algorithms of Numerical Mathematics, Proceedings of Seminar. Dolní Maxov, June 8-13, 2014. Institute of Mathematics AS CR, Prague, 2015. pp. 207–214.

Persistent URL: http://dml.cz/dmlcz/702686

Programs and Algorithms of Numerical Matematics 17
J. Chleboun, P. Přikryl, K. Segeth, J. Šístek, T. Vejchodský (Eds.)
Institute of Mathematics AS CR, Prague 2015

NUMERICAL SIMULATION OF FREE-SURFACE FLOWS WITH SURFACE TENSION

Petr Sváček

Czech Technical University, Faculty of Mechanical Engineering
Dep. of Technical Mathematics, Karlovo nám. 13, Praha 2, Czech Republic
Petr.Svacek@fs.cvut.cz

Abstract

This paper focuses on the mathematical modelling and the numerical approximation of the flow of two immiscible incompressible fluids. The surface tension effects are taken into account and mixed boundary conditions are used. The weak formulation is introduced, discretized in time, and the finite element method is applied. The free surface motion is treated with the aid of the level set method. The numerical results are shown.

1. Introduction

The mathematical modelling of two-phase flows with the consideration of the free surface motion influenced by the surface tension is addressed in various scientific as well as technical applications. Such a problem is important both from the mathematical modelling point of view and also from the technical practice. Particularly, its numerical approximation is very challenging task, see among others [1], [2] or [3]. The approximation of the surface tension naturally can play a key role here.

In this paper, we consider the two-dimensional flow of two immiscible fluids, the problem is mathematically described and the variational formulation is introduced. For the discretization the finite element(FE) method is used. The free surface motion is realized using the level set method, cf. [7] or [5]. In the case of high surface tension, a modification of the standard FE method is required to avoid the spurious currents, see [6] or [1]. For the verification of the implemented method a benchmark problem is solved, cf. [3].

2. Mathematical description

Let us consider the computational domain $\Omega \subset \mathbb{R}^2$ with the Lipschitz continuous boundary $\partial\Omega$ with its mutually disjoint parts Γ_W, Γ_S, Γ_O. The domain is occupied at time t by two immiscible fluids, i.e. $\Omega = \Omega^A_{(t)} \cup \Omega^B_{(t)}$, the fluid A occupies $\Omega^A_{(t)}$ and the fluid B occupies $\Omega^B_{(t)}$, see Fig. 1. The interface between the two fluids is denoted

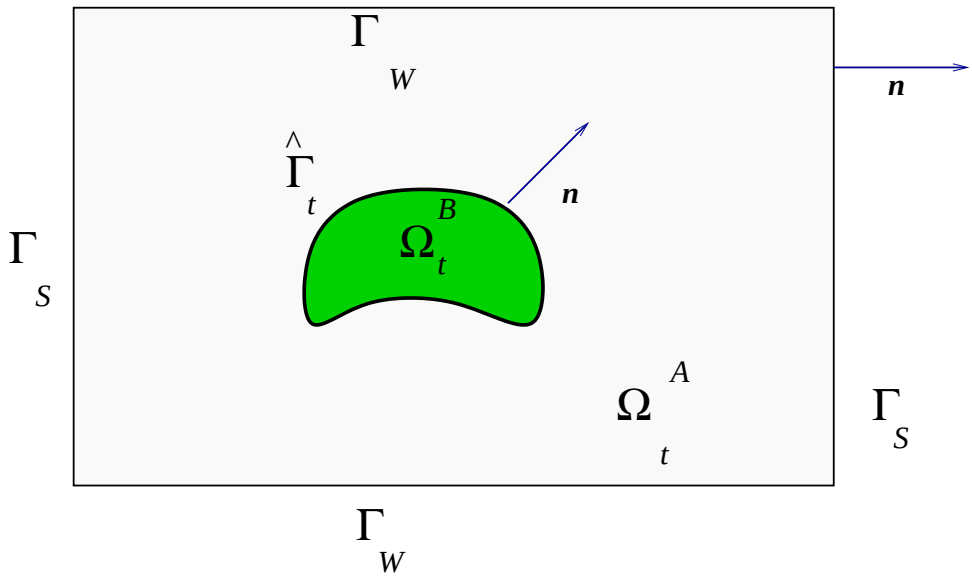

Figure 1: The computational domain Ω, its sub-domains $\Omega^A_{(t)}$ and $\Omega^B_{(t)}$, the interface $\hat{\Gamma}_t$ and the normal vector.

by $\hat{\Gamma}_t = \partial\Omega^A_{(t)} \cap \partial\Omega^B_{(t)}$. Further, we denote by $\Gamma^k_{W,t} = \Gamma_W \cap \partial\Omega^k_{(t)}$, $\Gamma^k_{S,t} = \Gamma_S \cap \partial\Omega^k_{(t)}$ and $\Gamma^k_{O,t} = \Gamma_O \cap \partial\Omega^k_{(t)}$ for $k = A$ or $k = B$.

The flow of the fluid A in the domain $\Omega^A_{(t)}$ is described by the incompressible system of Navier-Stokes equations

$$\frac{\partial\left(\rho^A \boldsymbol{u}^A\right)}{\partial t} + \rho^A(\boldsymbol{u}^A \cdot \nabla)\boldsymbol{u}^A - \nabla \cdot \boldsymbol{\sigma}^A = \rho^A \boldsymbol{f}, \qquad \nabla \cdot \boldsymbol{u}^A = 0, \tag{1}$$

where ρ^A denotes the constant fluid A density, $\boldsymbol{u}^A = \boldsymbol{u}^A(x,t)$ is its flow velocity defined for $x \in \Omega^A_{(t)}$ and $t \in [0,T)$, and $\boldsymbol{\sigma}^A$ is the Cauchy stress tensor given by $\boldsymbol{\sigma}^A = -p^A I + \mu^A(\nabla \boldsymbol{u}^A + \nabla^T \boldsymbol{u}^A)$, where $p^A = p^A(x,t)$ is the pressure and μ^A is the viscosity coefficient. Similarly, the flow of the fluid B in the domain $\Omega^B_{(t)}$ is governed by

$$\frac{\partial\left(\rho^B \boldsymbol{u}^B\right)}{\partial t} + \rho^B(\boldsymbol{u}^B \cdot \nabla)\boldsymbol{u}^B - \nabla \cdot \boldsymbol{\sigma}^B = \rho^B \boldsymbol{f}, \qquad \nabla \cdot \boldsymbol{u}^B = 0, \tag{2}$$

where ρ^B denotes the constant fluid B density, $\boldsymbol{u}^B = \boldsymbol{u}^B(x,t)$ is its flow velocity defined for $x \in \Omega^B_{(t)}$ and $t \in [0,T)$, and $\boldsymbol{\sigma}^B$ is the Cauchy stress tensor given by $\boldsymbol{\sigma}^B = -p^B I + \mu^B(\nabla \boldsymbol{u}^B + \nabla^T \boldsymbol{u}^B)$, where $p^B = p^B(x,t)$ is the pressure and μ^B is the viscosity coefficient. In eqs. (1-2) $\boldsymbol{f}$ denotes the gravitational acceleration (acting in the negative x_2 direction).

The motion of both fluids is then driven by the continuity equation

$$\frac{\partial \rho}{\partial t} + (\boldsymbol{u} \cdot \nabla)\rho = 0. \tag{3}$$

The domains $\Omega^A_{(t)}$ and $\Omega^B_{(t)}$ are then implicitly determined by the equations $\rho = \rho^A$ and $\rho = \rho^B$, respectively.

The initial conditions at time $t = 0$ are given $\boldsymbol{u}^A(x,0) = 0$, $\rho(x,0) = \rho^A$ for $x \in \Omega^A_{(0)}$ and $\boldsymbol{u}^B(x,0) = 0$, $\rho(x,0) = \rho^B$ for $x \in \Omega^B_{(0)}$. On the interface the following boundary conditions are specified on $\hat{\Gamma}_t$

$$a) \qquad \boldsymbol{u}^A = \boldsymbol{u}^B, \qquad b) \qquad \sigma^A \cdot \boldsymbol{n} - \sigma^B \cdot \boldsymbol{n} = \gamma\kappa\boldsymbol{n}, \tag{4}$$

where γ is the surface tension coefficient, κ denotes the curvature of the interface Γ_I and $\boldsymbol{n}$ here denotes the normal to the Γ_I pointing into $\Omega^B_{(t)}$. On the boundary $\partial\Omega$ the following boundary conditions are prescribed

$$\begin{array}{lllll}
a) & \boldsymbol{u}^A = 0 & \text{on } \Gamma^A_{W,t}, & \boldsymbol{u}^B = 0 & \text{on } \Gamma^B_{W,t}, \\
b) & \boldsymbol{u}^A \cdot \boldsymbol{n} = 0, \frac{\partial(\boldsymbol{u}^A \cdot \boldsymbol{t})}{\partial \boldsymbol{n}} = 0 & \text{on } \Gamma^A_{S,t}, & \boldsymbol{u}^B \cdot \boldsymbol{n} = 0, \frac{\partial(\boldsymbol{u}^B \cdot \boldsymbol{t})}{\partial \boldsymbol{n}} = 0 & \text{on } \Gamma^B_{S,t}, \\
c) & \boldsymbol{\sigma}^A \cdot \boldsymbol{n} = 0 & \text{on } \Gamma^A_{O,t}, & \boldsymbol{\sigma}^B \cdot \boldsymbol{n} = 0 & \text{on } \Gamma^B_{O,t},
\end{array} \tag{5}$$

where $\boldsymbol{n}$ denotes the unit outward normal to the boundary of Ω, and $\boldsymbol{t}$ is the unit tangent vector to the boundary of Ω.

3. Variational formulation

In order to introduce the weak formulation, we start with the definition of the function space $Q = L^2(\Omega)$ for the pressure and $\boldsymbol{V}$ the function space for the velocity, where $\boldsymbol{V} = \{\boldsymbol{v} \in \boldsymbol{H}^1(\Omega) : \boldsymbol{v} = 0 \text{ on } \Gamma_W, \boldsymbol{v} \cdot \boldsymbol{n} = 0 \text{ on } \Gamma_S\}$. Now, let us take the test function $\boldsymbol{v} \in \boldsymbol{V}$ and multiply the first equations in (1-2) by $\boldsymbol{v}$, integrate over Ω, use Green's theorem, apply the boundary conditions (5b-c) and use the interface condition (4b). We get

$$\begin{aligned}
&\int_{\Omega^A_{(t)}} \rho^A \left(\frac{\partial \boldsymbol{u}^A}{\partial t} + (\boldsymbol{u}^A \cdot \nabla)\boldsymbol{u}^A \right) \cdot \boldsymbol{v} + \boldsymbol{\sigma}^A \cdot (\nabla \boldsymbol{v}) \,\mathrm{d}x - \int_{\Omega^A_{(t)}} \rho^A \boldsymbol{f} \cdot \boldsymbol{v} \,\mathrm{d}x \quad + \\
&\int_{\Omega^B_{(t)}} \rho^B \left(\frac{\partial \boldsymbol{u}^B}{\partial t} + (\boldsymbol{u}^B \cdot \nabla)\boldsymbol{u}^B \right) \cdot \boldsymbol{v} + \boldsymbol{\sigma}^B \cdot (\nabla \boldsymbol{v}) \,\mathrm{d}x - \int_{\Omega^B_{(t)}} \rho^B \boldsymbol{f} \cdot \boldsymbol{v} \,\mathrm{d}x \quad = \quad \int_{\hat{\Gamma}_t} \gamma\kappa\boldsymbol{n} \cdot \boldsymbol{v} \,\mathrm{d}S.
\end{aligned} \tag{6}$$

Formulation (6) can be written in a more compact form using the Heaviside function $H(x,t)$ defined as $H(x,t) = 1$ for $x \in \Omega^A_{(t)}$, $H(x,t) = 0$ for $x \in \Omega^B_{(t)} \cup \hat{\Gamma}_t$. The density and the viscosity functions then are defined by $\rho(x,t) = \rho^A H(x,t) + (1 - H(x,t))\rho^B$ and $\mu(x,t) = \mu^A H(x,t) + (1 - H(x,t))\mu^B$, respectively. Further, the functions $\boldsymbol{u} = \boldsymbol{u}(x,t)$ and $p = p(x,t)$ can be defined by

$$\boldsymbol{u}(x,t) = \begin{cases} \boldsymbol{u}^A(x,t) & \text{for } x \in \overline{\Omega^A_{(t)}}, \\ \boldsymbol{u}^B(x,t) & \text{for } x \in \overline{\Omega^B_{(t)}}, \end{cases} \qquad p(x,t) = \begin{cases} p^A(x,t) & \text{for } x \in \overline{\Omega^A_{(t)}} \setminus \hat{\Gamma}_t, \\ p^B(x,t) & \text{for } x \in \overline{\Omega^B_{(t)}} \setminus \hat{\Gamma}_t. \end{cases}$$

Using this notation, the equation (6) then can be written as

$$\int_\Omega \rho \left(\frac{\partial \boldsymbol{u}}{\partial t} + (\boldsymbol{u} \cdot \nabla)\boldsymbol{u} \right) \cdot \boldsymbol{v} + \boldsymbol{\sigma} \cdot (\nabla \boldsymbol{v}) \,\mathrm{d}x = \int_{\hat{\Gamma}_t} \gamma\kappa\boldsymbol{n} \cdot \boldsymbol{v} \,\mathrm{d}S + \int_\Omega \rho \boldsymbol{f} \cdot \boldsymbol{v} \,\mathrm{d}x, \tag{7}$$

where $\boldsymbol{\sigma}$ is the Cauchy stress tensor given by $\boldsymbol{\sigma} = -pI + \mu(\nabla \boldsymbol{u} + \nabla^T \boldsymbol{u})$. Using the Dirac delta function $\delta_{\hat{\Gamma}_t}$ of the interface $\hat{\Gamma}_t$ the equation (7) can be written in the form

$$\rho \frac{\partial \boldsymbol{u}}{\partial t} + \rho(\boldsymbol{u} \cdot \nabla)\boldsymbol{u} - \nabla \cdot \boldsymbol{\sigma} = \rho \boldsymbol{f} + \gamma \kappa \boldsymbol{n} \delta_{\hat{\Gamma}_t}. \tag{8}$$

Surface tension. In order to treat the surface tension term, we start with its weak reformulation. Let us define the tangent derivative ∇_Γ as $\nabla_\Gamma g = \nabla g - (\boldsymbol{n} \cdot \nabla g)\boldsymbol{n}$ and the Laplace-Beltrami operator $\triangle_\Gamma = \nabla_\Gamma \cdot \nabla_\Gamma$. Now, using the relation $\kappa \boldsymbol{n} = \triangle_\Gamma \boldsymbol{x}$ and applying the integration by parts on $\hat{\Gamma}_t$ we get

$$\int_{\hat{\Gamma}_t} \gamma \kappa \boldsymbol{n} \cdot \boldsymbol{v} \, \mathrm{d}S = -\int_{\hat{\Gamma}_t} \gamma (\nabla_\Gamma \boldsymbol{x}) \cdot (\nabla_\Gamma \boldsymbol{v}) \, \mathrm{d}S, \tag{9}$$

where for the sake of simplicity it was assumed that $\hat{\Gamma}_t$ is a closed curve.

Level set equation. Furthermore, to treat the motion of the free surface $\hat{\Gamma}_t$ the *level set* method is applied. First, the initial condition for the level set function $\phi = \phi(x,t)$ is prescribed by $\phi(x,0) = \mathrm{dist}(x, \hat{\Gamma}_0) > 0$ for $x \in \Omega^A_{(0)}$, $\phi(x,0) = -\mathrm{dist}(x, \hat{\Gamma}_0) < 0$ for $x \in \Omega^B_{(0)}$, and $\phi(x,0) = 0$ for $x \in \hat{\Gamma}_0$. The motion of the interface $\hat{\Gamma}_t$ is then realized by forcing the function ϕ to solve the equation

$$\frac{\partial \phi}{\partial t} + \boldsymbol{u} \cdot \nabla \phi = 0, \tag{10}$$

which guarantees that the interface is moving with the velocity $\boldsymbol{u}$. Now, the Heaviside function $H(x,t)$ is defined using the sign of the level set function $\phi(x,t)$. Taking into account the level set equation (10) and the definition of the function $\rho(x,t)$, the continuity equation (3) is formally satisfied.

4. Numerical approximation

Flow step. For simplicity, let us consider the equidistant partition of the time interval $[0,T)$ given by $t_n = n\Delta t$, where $n = 0, 1, \ldots, N$ and $\Delta t = T/N$. Let us denote by $\boldsymbol{u}^{(n)}$, $p^{(n)}$, $\phi^{(n)}$, ρ^n and μ^n approximations of the velocity, the pressure the level set function, the density and the viscosity at the time instant t_n, respectively. Let us approximate the time derivative by the backward Euler formula, i.e.

$$\frac{\partial \boldsymbol{u}}{\partial t}|_{t=t_{n+1}} \approx \frac{\boldsymbol{u}^{(n+1)} - \boldsymbol{u}^{(n)}}{\Delta t}, \qquad \frac{\partial \phi}{\partial t}|_{t=t_{n+1}} \approx \frac{\phi^{(n+1)} - \phi^{(n)}}{\Delta t}.$$

Let us assume that $\boldsymbol{u}^{(n)}$, $p^{(n)}$, $\phi^{(n+1)}$, μ^{n+1} and $\rho^{(n+1)}$ are already known. Then the time discretized weak formulation of (8) reads: Find $\boldsymbol{u} = \boldsymbol{u}^{n+1} \in \boldsymbol{V}$ and $p = p^{n+1} \in Q$ such that

$$\begin{aligned} &\int_\Omega \rho^{n+1}(x) \left(\frac{\boldsymbol{u} - \boldsymbol{u}^n}{\Delta t} + (\boldsymbol{u} \cdot \nabla)\boldsymbol{u} \right) \cdot \boldsymbol{v} - p(\nabla \cdot \boldsymbol{v}) + \mu^{n+1}(x) \nabla \boldsymbol{u} \cdot \nabla \boldsymbol{v} \, \mathrm{d}x \\ &\quad + \int_\Omega (\nabla \cdot \boldsymbol{u}) q \, \mathrm{d}x = -\int_{\hat{\Gamma}^{n+1}} \gamma (\nabla_\Gamma \boldsymbol{x}) \cdot (\nabla_\Gamma \boldsymbol{v}) \, \mathrm{d}S + \int_\Omega \rho^{n+1}(x) \boldsymbol{f} \cdot \boldsymbol{v} \, \mathrm{d}x \end{aligned} \tag{11}$$

holds for all $\boldsymbol{v} \in \boldsymbol{V}$ and $q \in Q$. In the practical computations we assume that the domain Ω is a polygonal and the spaces $\boldsymbol{V}$ and Q are approximated by the FE subspaces $\boldsymbol{V}_h$ and Q_h defined over an admissible triangulation $\mathcal{T}_h$, respectively. For the approximation the well-known Taylor-Hood FE are used, i.e. the velocity is sought in the space $\boldsymbol{V}_h = [H_h]^2 \subset \boldsymbol{V}$, where

$$H_h = \{\phi \in C(\overline{\Omega}); \phi|_K \in P_2(K) \text{ for each } K \in \mathcal{T}_h\}, \tag{12}$$

where $P_k(K)$ denotes the space of all polynomials on K of degree less or equal to k. Next, the pressure (as well as the level set function) is approximated in the space

$$Q_h = \left\{\phi \in C(\overline{\Omega}) : \ \phi|_K \in P_1(K) \text{ for each } K \in \mathcal{T}_h\right\}. \tag{13}$$

The discrete flow problem then reads: Find $\boldsymbol{u}_h = \boldsymbol{u}_h^{n+1} \in \boldsymbol{V}_h$ and $p_h = p_h^{n+1}$ such that equation (11) holds for any test function $\boldsymbol{v} := \boldsymbol{v}_h \in \boldsymbol{V}_h$ and $q := q_h \in Q_h$. In order to treat the discontinuity of the pressure due to the presence of the surface tension the extended finite element method (XFEM) is applied, see e.g. [6].

Extended finite element method. The XFEM enlarges the original FE space Q_h using the localization of an enrichment function. For the localization the original base functions of Q_h are used, i.e. we denote the index set $\mathcal{J} = \{1, \dots, n\}$, $n = \dim Q_h$ and the mesh nodes by $\boldsymbol{x}_j$, $j \in \mathcal{J}$. The nodal base functions are then denoted by $q_i \in Q_h$, $i \in \mathcal{J}$ and satisfy $q_i(\boldsymbol{x}_j) = \delta_{ij}$. The $\mathcal{J}'$ is the subset of all the neighbours of the interface $\hat{\Gamma}_t$, i.e. $\mathcal{J}' = \{j \in \mathcal{J} : \operatorname{supp} q_j \cap \hat{\Gamma}_t \neq \emptyset\}$. We shall use the discontinuous enrichment function $H_\Gamma(\boldsymbol{x})$ given as the Heaviside function $H_\Gamma(\boldsymbol{x}) = H(\boldsymbol{x}, t_{n+1})$. Now, the enrichment of the space Q_h is made using the discontinuous base functions q_j^{xfe} defined by $q_j^{xfe}(\boldsymbol{x}) = q_j(\boldsymbol{x})\,(H_\Gamma(\boldsymbol{x}) - H_\Gamma(\boldsymbol{x}_j))$. Here, $H_\Gamma(\boldsymbol{x}_j)$ can be left out from the right hand side as this only adds a constant multiple of the continuous base function $q_j(\boldsymbol{x})$. On the other hand, this term makes the function $q_j^{xfe}(\boldsymbol{x})$ being zero at every node $\boldsymbol{x}_i$, $i \in \mathcal{J}$ and also makes the support of $q_j^{xfe}(\boldsymbol{x})$ localized only to the elements containing the interface $\hat{\Gamma}_t$, which simplifies the practical discretization of the problem. The FE space Q_h is then replaced by the extended FE space $Q_h^{xfe} = Q_h \oplus \operatorname{span}\{q_j^{xfe} : j \in \mathcal{J}'\}$.

Level set step and coupled problem. Eq. (10) is time discretized, weakly formulated and the standard Galerkin FE method is employed, leading to the discrete system

$$\mathbb{M}(\Phi^{(n+1)} - \Phi^{(n)}) + \Delta t\, \mathbb{K}\Phi^{(n+1)} = 0, \tag{14}$$

where $\mathbb{M}$ is the consistent mass matrix, the matrix $\mathbb{K}$ represents the convection and $\Phi^{(k)} = \left(\phi^{(k)}(\boldsymbol{x}_i)\right)_{i \in \mathcal{J}}$ denotes the nodal values of the level set function. In order to obtain a stable scheme, the algebraic flux corrections can be applied, see [4]. Nevertheless, in the considered case of a continuous level set function φ, this is mostly equivalent to the Galerkin method (at least for a limited time period). It is also known, that for the level set method a re-initialization step is needed to

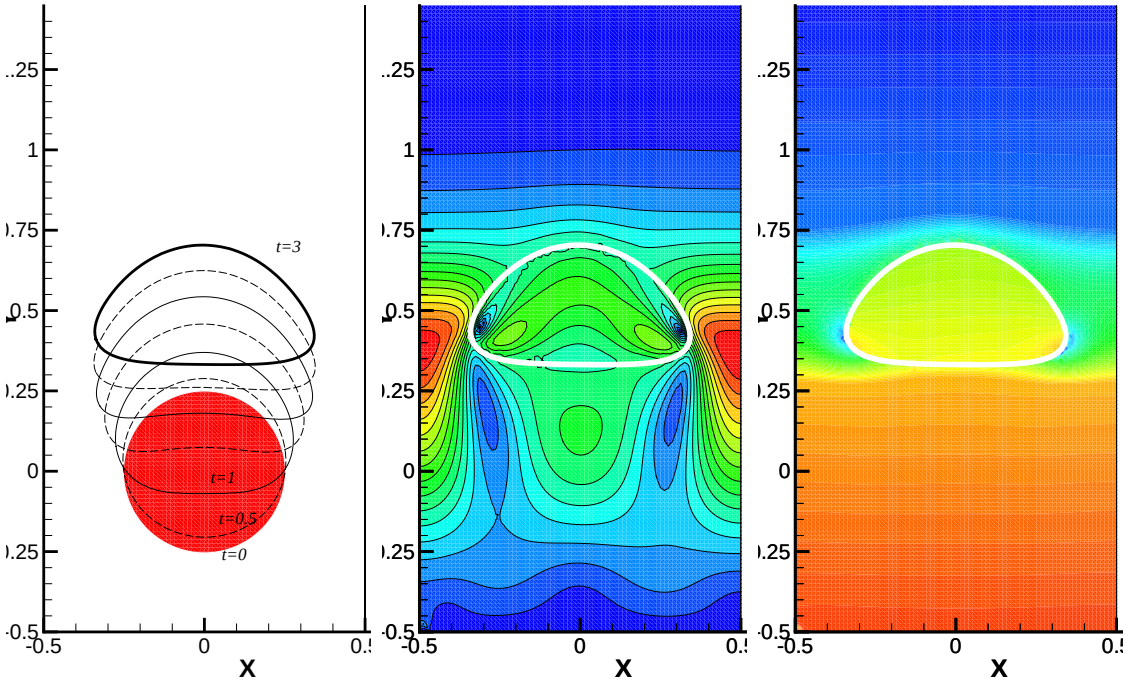

Figure 2: The result of the rising bubble case: The shape of the interface at time instant $t \in \{0, 0.5, 1, 1.5, 2, 3\}$ (on the left), the velocity magnitude isolines (middle), and the pressure isolines (on the right).

maintain the distance like property, see also [3]. Thus we simply use the Galerkin FE approximations and perform the re-initialization step every 5-40 iterations.

The solution of the coupled problem is then performed by the de-coupled algorithm: Assume that the approximations of $\boldsymbol{u}^n$, p^n, ϕ^n, ρ^n, μ^n and $\hat{\Gamma}^{(n)}$ are already known.

I. Solve (14) using the flow velocity $\boldsymbol{u}^n$ to determine ϕ^{n+1}. Perform the re-initialization if needed.

II. Using the approximation ϕ^{n+1} determine ρ^{n+1}, μ^{n+1} and $\hat{\Gamma}^{n+1}$.

III. Solve (11) for approximation of flow velocity $\boldsymbol{u}^{n+1}$ and p^{n+1}.

IV. Set n:= n + 1 and go to I.

5. Numerical results

The numerical results are shown for the case of a rising bubble considered in [3], where the following values were used $\rho^A = 1000\,\mathrm{kg\,m^{-3}}$, $\rho^B = 100\,\mathrm{kg\,m^{-3}}$, $\mu_A = 10\,\mathrm{Pa\,s}$, $\mu_B = 1\,\mathrm{Pa\,s}$, $\boldsymbol{f} = (0, -0.98)\,\mathrm{m\,s^{-2}}$ and $\gamma = 24.5\,\mathrm{N/m}$. The height of the computational domain is $H = 2\,\mathrm{m}$ and width is $W = 1\,\mathrm{m}$. The fluid B is originally

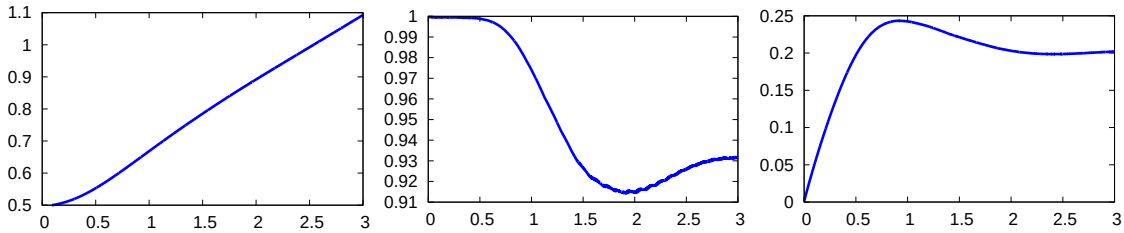

Figure 3: The quantitative results for the rising bubble case: The graphs of the center of mass T_y, the circularity C and the rise velocity V from the left to the right, respectively.

located in the circle of the diameter 0.5 m, whose center is displaced by 0.5 m up from the bottom of the domain. The boundary Γ_W contains the bottom and top of the domain, whereas Γ_S includes the rest of the boundary (i.e. $\Gamma_O = \emptyset$). Due to the gravity force, the fluid B with the lower density starts to rise, which also leads to a shape deformation. However, after some time the fluid B - due to the high value of the surface tension - develops a more stable shape, which keeps rising undeformed, see Fig. 2. The computations were performed on a triangular mesh with an equidistant partition and the spatial step $h = 1/40$ (the coarsest mesh used in [3]). The time step used in the computation was $\Delta t = 0.002$. The motion of the domain $\Omega^B_{(t)}$ with the area $\mathcal{A}(t)$ was tracked in terms of the $y-$coordinate of the center of mass $T_y(t) = \int_{\Omega^B_{(t)}} x_2 \,\mathrm{d}x/\mathcal{A}(t)$, the circularity defined by $C(t) = 2\sqrt{\pi\mathcal{A}(t)}/\int_{\partial\Omega^B_{(t)}} 1 \,\mathrm{d}S$ and the rise velocity $V = \int_{\Omega^B_{(t)}} u_2 \,\mathrm{d}x/\mathcal{A}(t)$. In order to verify the presented numerical method the values of T_y, C and V were computed at every time instant. The graphs of T_y, C and V in dependence on time shown in Figure 3 agrees well with the results in [3]. The quantitative comparison of the referenced values presented in [3] is shown in Table 1, where $T_y(3)$ is the mass center location at time $t = 3\,\mathrm{s}$, $C_{\min}$ denotes the minimal circularity, $V_{\max}$ denotes the maximal rise velocity, $t(C = C_{\min})$ and $t(V = V_{\max})$ are the time instants of their occurrence, respectively.

6. Conclusion

The detailed mathematical description of the motion of two immiscible fluids flow was presented, where the surface tension was approximated using its weak reformulation. The first order time discretization was used and the finite element method was used for the space discretization. The XFEM was employed to capture correctly the discontinuity of the pressure along the surface caused by the surface tension. The solution of the flow problem was coupled with the FEM applied for solution of the transport equation for the level set function. The decoupled strategy was used for the solution of the coupled problem. The presented numerical method was applied for approximation of the benchmark [3]. The data from the numerical simulations shows very good agreement with the reference values even though here only the first

	$T_y(3)$	$C_{\min}$	$t(C = C_{\min})$	$V_{\max}$	$t(V = V_{\max})$
ref. [3]	1.0813	0.9013	1.9041	0.2417	0.9213
present study	1.0801	0.9025	1.898	0.2421	0.92

Table 1: The quantitative results for the rising bubble case: the comparison of the computed and the reference quantities.

order in time discretization was used. The obtained numerical results verify the applied numerical method and its usability for approximation of flows influenced by the surface tension.

Acknowledgements

This work was supported by grant No. 13-00522S of the Czech Science Foundation.

References

[1] Barrett, J. W., Garcke, H., and Nürnberg, R.: Eliminating spurious velocities with a stable approximation of viscous incompressible two-phase Stokes flow. Compu. Methods Appl. Mech. Engrg. **267** (2013), 511–530.

[2] Hirt, C. W. and Nichols, B. D.: Volume of fluid (VOF) method for the dynamics of free boundaries. J. Comput. Phys. **39** (1981), 201–225.

[3] Hysing, S. et al.: Quantitative benchmark computations of two-dimensional bubble dynamics. Internat. J. Numer. Methods Fluids **60** (2009), 1259–1288.

[4] Kuzmin, D.: On the design of general-purpose flux limiters for finite element schemes. I. Scalar convection. J. Comput. Phys. **219**(2), 2006, 513–531.

[5] Ransau, S. R.: Solution methods for incompressible viscous free surface flows: A literature review. Tech. Rep. 3/2002, Norwegian University of Science and Technology, Trondheim, 2002.

[6] Sauerland, H. and Fries, T. P.: The stable XFEM for two-phase flows. Comput. & Fluids **87** (2013), 41–49.

[7] Sethian, J. A.: *Level set methods and fast marching methods.* Cambridge Monograph on Applied and Computational Mathematics, Cambridge University Press, Cambridge, U.K., 1999, 2^{nd} edn.